

# Robust Channel Estimation for Optical Wireless Communications Using Neural Network

Dianxin Luan, *Graduated Student Member, IEEE*, John Thompson, *Fellow, IEEE*

**Abstract**—Optical Wireless Communication (OWC) has gained significant attention due to its high-speed data transmission and throughput. Optical wireless channels are often assumed to be flat, but we evaluate frequency selective channels to consider high data rate optical wireless or very dispersive environments. To address this for optical scenarios, this paper presents a robust channel estimation framework with low-complexity to mitigate frequency-selective effects, then to improve system reliability and performance. This channel estimation framework contains a neural network that can estimate general optical wireless channels without prior channel information about the environment. Based on this estimate and the corresponding delay spread, one of several candidate offline-trained neural networks will be activated to predict this channel. Simulation results demonstrate that the proposed method has improved and robust normalized mean square error (NMSE) and bit error rate (BER) performance compared to conventional estimation methods while maintaining computational efficiency. These findings highlight the potential of neural network solutions in enhancing the performance of OWC systems under indoor channel conditions.

**Index Terms**—Channel estimation, Deep learning, Orthogonal frequency-division multiplexing (OFDM), Optical wireless communications (OWC).

## I. INTRODUCTION

WIRELESS communications are critical for current applications but largely rely on radio frequency (RF) systems. Compared to RF, optical wireless communications (OWC) are able to offer higher air interface rates and lower transmission power. This ensures OWC is a competitive solution compared to RF, especially for indoor wireless communications. Therefore, OWC has emerged as a potential technology for next-generation wireless networks, offering license-free spectrum, high bandwidth and inherent security [1]. By leveraging visible light, infrared, or ultraviolet bands, OWC systems—including visible light communication (VLC), light-fidelity (Li-Fi), and free-space optical (FSO) links—are being deployed in diverse applications, from indoor networks to underwater communications [2]. However, the performance of OWC systems is dependent on accurate channel state information (CSI). Time-varying characteristics induced by user orientations and multipath propagation require robust channel estimation techniques to ensure reliable data transmission. Conventional techniques such as least-squares (LS) and minimum mean square error (MMSE) are widely applied for wireless applications. Due to the inadequacy of conventional methods in meeting current demands, neural network solutions have been investigated to enhance performance and reliability [3]–[7]. For optical wireless channels, the paper [8] proposes a novel channel model for optical wireless scattering com-

munication and compares MMSE receiver with a maximum-likelihood sequence detection (MLSD) solution. To achieve better performance, a neural network approach is proposed in [9] that tackles channel estimation in underwater wireless optical communication (UWOC) systems, which improves both reliability and data rates in complex underwater environments. In addition, the papers [10] [11] investigate channel estimation neural networks for different optical scenarios. However, wireless optical channels are typically characterized by a dominant line-of-sight (LOS) component accompanied by several non-line-of-sight (NLOS) multipath components arising from reflections off walls, ceilings and other surfaces. Conventionally, the LOS component is tens of decibels stronger than the reflection components [12], leading to a common assumption that the optical wireless channel is often flat.

In this paper, we propose an adaptive neural network solution to estimate wireless optical channels robustly and reduce the bit errors at the receiver end. This adaptive neural network estimates the OWC channel then choose the most suitable neural network to achieve overall improvement. For simulations, this paper deploys a ray tracing simulator for realistic modeling of the environment, which shows frequency-selective scenarios for orthogonal frequency-division multiplexing (OFDM) waveforms, even when the reflection path has only a very small gain.

Section. II presents the system settings and conventional channel estimation methods. Section. III shows the frequency selective property of wireless optical channels and then introduces the proposed adaptive neural network solution. Section. IV presents key simulation results comparing the different methods. Section. V summarizes the key findings of this paper. The simulation code for this deployed OWC channel is available at <https://github.com/dianixn/OWC-Channels>.

## II. SYSTEM SETTINGS AND CHANNEL MODEL

This paper considers an uncoded DCO-OFDM system for indoor transmission, where intensity modulation and direct detection (IM-DD) of the optical carrier using an incoherent light source is implemented. Each slot consists of  $N_f$  subcarriers and  $N_s$  OFDM symbols. The frequency-domain allocation for the demodulation reference signal comprises 4 pilot symbols which are the 3<sup>rd</sup>, 6<sup>th</sup>, 9<sup>th</sup> and 12<sup>th</sup> OFDM symbols. For each pilot OFDM symbol, the indices of the pilot subcarriers start from the first subcarrier and are spaced by  $L_s$  subcarriers and the remaining subcarriers are set to 0 for the first half subcarriers. All of the data subcarriers in the data OFDM symbols are assigned 64 Quadrature Amplitude Modulation

(QAM) modulated symbols. For each OFDM symbol  $s(i)$ , complex baseband signals are constrained to have Hermitian symmetry, i.e.  $\forall i \in [0, N_f - 1], s(i) = s^*(N_f - i)$  for the second half subcarriers of each OFDM symbol. The frequency-domain OFDM symbols are then obtained from the inverse fast Fourier transform (IFFT). The cyclic prefix (CP) with length of  $L_{CP}$  is inserted and a DC bias is applied to ensure the transmitted signal positive. For OWC system, we consider a block-fading channel that retains constant over each slot which has an impulse response of

$$g(t) = h_{\text{LOS}}\delta(t) + \sum_{i=1}^{M-1} h_{\text{NLOS}}^i \delta(t - \tau_m T_s), \quad (1)$$

where  $h_{\text{LOS}}$  is the LOS path gain and  $h_{\text{NLOS}}^m$  is the NLOS path gain for the  $m$ th path, which are real and nonnegative.  $\tau_m$  is the reflection delay normalized by the sampling period  $T_s$ . We only take into account specular reflections in this paper because diffuse reflections have a much smaller path power than that of diffuse path. The LOS and NLOS links are given by [13], [14]

$$h_{\text{LOS}} = \begin{cases} \frac{A((k+1)\cos^k(\phi)\cos(\theta))}{2\pi d^2}, & \theta \in [0, \varphi_{\frac{1}{2}}] \\ 0, & \text{otherwise} \end{cases}, \quad (2)$$

$$h_{\text{NLOS}} = \alpha \frac{A((k+1)\cos^k(\phi_{Tx})\cos(\theta_{Tx}))}{2\pi d_{Tx}^2}, \quad (3)$$

where  $k = \frac{-\ln(2)}{\ln(\cos(\Phi_{\frac{1}{2}}))}$ .  $A$  is the collection area of the photodiode (PD),  $\Phi_{\frac{1}{2}}$  is the transmitter semi-angle,  $\varphi_{\frac{1}{2}}$  is the FOV semi-angle of the receiver and  $\alpha$  is the surface reflection coefficient of the wall.  $\theta, \phi$  is the angle of incidence and emergence with respect to the receiver detector direction, and  $d$  is the distance between the transmitter and the receiver. For the specular reflection path,  $\theta_{Tx}, \phi_{Tx}$  is the angle of incidence and emergence from the image position of the transmitter to the receiver detector direction,  $d_{Tx}$  is the distance between the transmitter image and the receiver. By removing the CP and then applying the FFT operation, the received signal  $\mathbf{Y} \in \mathbb{C}^{N_f \times N_s}$ , can be represented by

$$\mathbf{Y} = \mathbf{H} \circ \mathbf{X} + \mathbf{W}, \quad (4)$$

where  $\mathbf{X}, \mathbf{H} \in \mathbb{C}^{N_f \times N_s}$  are the Discrete Fourier Transforms of the transmitted signal and the channel impulse responses. The matrix  $\mathbf{W}$  denotes the sum of frequency-domain ambient light shot and thermal noises, modeled as i.i.d. additive white Gaussian noise (AWGN) with a variance of  $\delta^2 = \delta_{\text{slot}}^2 + \delta_{\text{thermal}}^2$  [15]. The operator  $\circ$  represents the Hadamard product. If the maximum path delay is less than the duration of the CP, the received pilot signal is extracted to provide a channel reference for the complete packet. Conventionally, the LS estimate is calculated by  $\hat{\mathbf{H}}^{\text{LS}} = \mathbf{Y}_p / \mathbf{X}_p$  where  $\mathbf{Y}_p$  is the received pilot signal and  $\mathbf{X}_p$  is the transmitted pilot signal for a pilot OFDM symbol. Then  $\hat{\mathbf{H}}^{\text{LS}}$  is interpolated linearly for complete channel estimate  $\hat{\mathbf{H}}_{\text{Slot}}^{\text{LS}}$ . To reduce the mean square

error (MSE) of the LS estimate, the linear MMSE solution is given by

$$\hat{\mathbf{H}}^{\text{MMSE}} = \mathbf{R}_{\mathbf{H}\mathbf{H}_p} (\mathbf{R}_{\mathbf{H}_p\mathbf{H}_p} + \delta^2 \mathbf{I})^{-1} \hat{\mathbf{H}}^{\text{LS}}, \quad (5)$$

where  $\mathbf{R}_{\mathbf{H}\mathbf{H}_p}$  is the cross-correlation matrix between the actual channel matrix and the actual channel matrix at the pilot positions,  $\mathbf{R}_{\mathbf{H}_p\mathbf{H}_p}$  is the autocorrelation matrix of  $\mathbf{H}_p$  and  $\mathbf{I}$  is the identity matrix. Then  $\hat{\mathbf{H}}^{\text{MMSE}}$  is replicated for the whole slot to obtain  $\hat{\mathbf{H}}_{\text{Slot}}^{\text{MMSE}}$ . After equalizing the channel distortion, the processed signal is decoded to predict the bit-level data at the receiver end.

### III. ROBUST CHANNEL ESTIMATION FOR WIRELESS OPTICAL CHANNELS

In this section, we will show the frequency selective property of optical wireless channels, and then propose an adaptive neural network solution to estimate randomly generated channels.

#### A. Problem formulation

Typically, the optical wireless channel is assumed to be flat but the sampled channel impulse response possibly has multiple taps for OFDM waveform. Transferring equ. (1) into the frequency domain and then sampling this continuous expression, the  $k$ th channel gain and the corresponding channel impulse response are shown above. Equ. (7) shows that the sampled channel impulse response exhibits time dispersion characteristics due to the reflection path. This possibly results in weak frequency selective scenarios as shown in Fig. 1.

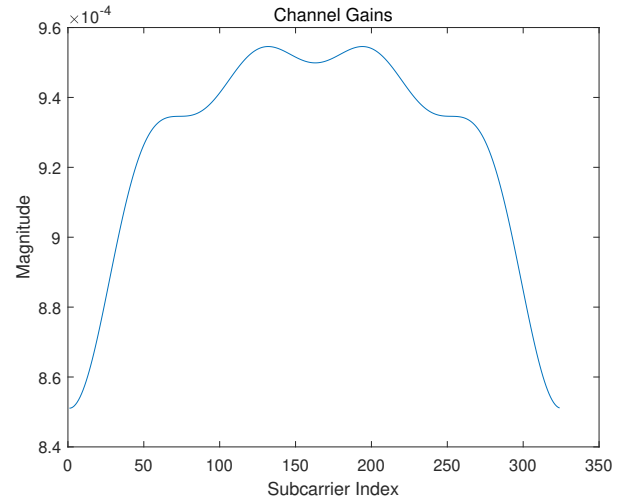


Fig. 1. Example of a two-path optical channel where the magnitude of the reflection path is tens dB less than that of the LOS path. As shown in this figure, the magnitude of each channel gain varies among subcarriers.

#### B. Robust and adaptive channel estimation solutions

To address this, a good channel estimator is required to compensate for this effect. In this paper, we propose a robust and adaptive channel estimation solution for optical channels. We select more representative channel samples for training

$$\mathbf{H}_k = h_{\text{LOS}} + \sum_{i=1}^{M-1} h_{\text{NLOS}} \frac{e^{-j \frac{2\pi}{N_f} k (\tau_i - \frac{N_f-1}{2})} \sin\left(\frac{\pi}{N_f} (2N_f \tau_i - k)\right)}{\sin\left(\frac{\pi}{N_f} k\right)}, \quad (6)$$

$$\mathbf{h}(n) = h_{\text{LOS}} \delta(n) + \sum_{i=1}^{M-1} h_{\text{NLOS}} \frac{\left(\sin\left(\frac{\pi}{N_f} (n + (2N_f - 1)\tau_i)\right) - \sin\left(\frac{\pi}{N_f} (n - \tau_i)\right)\right)}{2 \sin\left(\frac{\pi}{N_f} (\tau_i - n)\right)}. \quad (7)$$

neural networks to adapt to optical channels with low delay spreads (LDS), medium delay spreads (MDS) and high delay spreads (HDS), and then use the channel prediction from a particular neural network to precisely distinguish the delay spread of the optical channel being predicted. According to this classifier, the system will decide to activate one of these three trained neural networks for estimation.

In this paper, we deploy InterpolateNet [16] as an example neural network. It is a low-complexity convolutional neural network with only 9,442 tunable parameters, which deploys bilinear interpolation layer to resize the in-processing features. InterpolateNet achieves the mapping of  $\mathbf{H}^{\text{DNN}} = \mathcal{F}_P(\mathbf{H}^{\text{LS}})$  with a certain set parameters  $P$  where  $\mathbf{H}^{\text{DNN}} \in \mathbb{C}^{N_f}$  is the channel estimate for one OFDM symbol. This prediction will be replicated for each OFDM symbol to obtain  $\mathbf{H}_{\text{Slot}}^{\text{DNN}} \in \mathbb{C}^{N_f \times N_s}$  for the complete packet. We train three InterpolateNet networks individually with LDS, MDS and HDS channel samples, which have tunable parameters of  $\mathbf{P}_{\text{LDS}}$ ,  $\mathbf{P}_{\text{MDS}}$  and  $\mathbf{P}_{\text{HDS}}$ . For example, as shown in Fig. 2, InterpolateNet with  $\mathbf{P}_{\text{HDS}}$  is trained on the optical channels that have a sampled power delay profile (PDP) above that of  $\mathbf{h}_{\text{HDS}}$  (red curve), which represents HDS scenarios. InterpolateNet with  $\mathbf{P}_{\text{LDS}}$  is trained on the channel samples that have lower PDP values than  $\mathbf{h}_{\text{LDS}}$  (blue curve), which is the worst case LDS scenario. InterpolateNet with  $\mathbf{P}_{\text{MDS}}$  is trained on the optical channels between these two chosen channels. The choice of the values of  $\mathbf{h}_{\text{LDS}}$  and  $\mathbf{h}_{\text{HDS}}$  is based on clustering environment measurement for implementation.

As shown in [17], InterpolateNet with  $\mathbf{P}_{\text{HDS}}$  should generalize well to most of the possible scenarios and provide a good estimation for them. Therefore, as described in Algorithm. 1, we use the estimate from this neural network to calculate the channel impulse response. This paper predicts the channel impulse response by using the IFFT operation and  $\mathbf{H}^{\text{DNN}}$  from the first step. The proposed algorithm then compares  $\mathbf{h}_{\text{HDS}}$  and  $\mathbf{h}_{\text{LDS}}$  to decide if switch to another set of parameters for a more precise estimation.

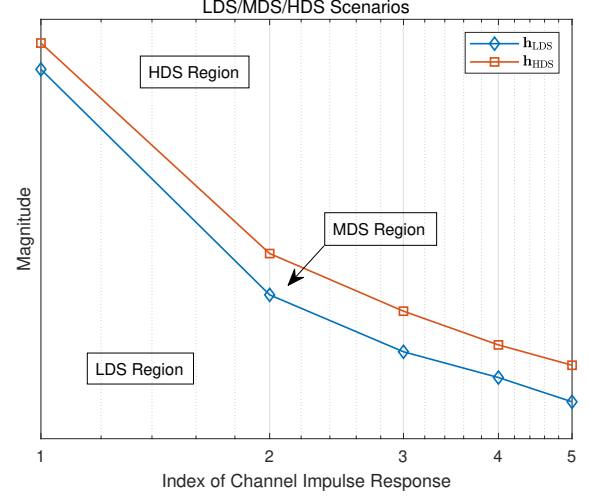


Fig. 2. Example of a possible set of  $\mathbf{h}_{\text{LDS}}$  and  $\mathbf{h}_{\text{HDS}}$ .

---

#### Algorithm 1 InterpolateNets Selection&Prediction

---

**Require:**  $\mathbf{h}_{\text{HDS}}, \mathbf{h}_{\text{LDS}}, \mathbf{P}_{\text{HDS}}, \mathbf{P}_{\text{MDS}}, \mathbf{P}_{\text{LDS}}, \mathcal{F}$

**Ensure:**  $\forall i \in [1 : L_{\text{CP}}], |\mathbf{h}_{\text{HDS}}(i)| > |\mathbf{h}_{\text{LDS}}(i)|$

- 1:  $\mathbf{H}^{\text{DNN}} \leftarrow \mathcal{F}_{\mathbf{P}_{\text{HDS}}}(\mathbf{H}^{\text{LS}})$
  - 2:  $\mathbf{h}_{\text{est}} \leftarrow$  Estimate time impulse response by  $\mathbf{H}^{\text{DNN}}$
  - 3:  $\mathbf{h}_{\text{abs}} \leftarrow \text{abs}(\mathbf{h}_{\text{est}})$
  - 4: **if**  $\forall i \in [1 : L_{\text{CP}}], \mathbf{h}_{\text{abs}}(i) < |\mathbf{h}_{\text{LDS}}(i)|$  **then**
  - 5:    $\mathbf{H}^{\text{DNN}} \leftarrow \mathcal{F}_{\mathbf{P}_{\text{LDS}}}(\mathbf{H}^{\text{LS}})$
  - 6: **else if**  $\forall i \in [1 : L_{\text{CP}}], \mathbf{h}_{\text{abs}}(i) < |\mathbf{h}_{\text{HDS}}(i)|$  **then**
  - 7:    $\mathbf{H}^{\text{DNN}} \leftarrow \mathcal{F}_{\mathbf{P}_{\text{MDS}}}(\mathbf{H}^{\text{LS}})$
  - 8: **else**
  - 9:   **Do Nothing**
  - 10: **end if**
- 

## IV. SIMULATION RESULTS

For the rest of this paper,  $M$  is assumed to be 2 which represents a two-path channel for common indoor OWC scenarios. Normalized mean square error (NMSE) is a key performance metric that evaluates the distance between the actual channel and the estimate of channel for each resource element in the slot, which is defined as

$$\text{NMSE}(\hat{\mathbf{H}}_{\text{Slot}}, \mathbf{H}) = \frac{\mathbb{E} \left\{ \left\| \hat{\mathbf{H}}_{\text{Slot}} - \mathbf{H} \right\|_F^2 \right\}}{\mathbb{E} \{ \left\| \mathbf{H} \right\|_F^2 \}}, \quad (8)$$

where  $\|\cdot\|_F^2$  is the Frobenius norm. The bit error ratio (BER) is another performance metric which refers to the ratio of bit errors per frame. For the settings of optical wireless channel, the hyper-parameters are given in Table. I. As the CP is shown to have a negligible impact on the electrical signal-to-noise ratio (SNR) requirement for optical systems [18], we consider environment SNRs from 15dB to 30dB in this paper. The

TABLE I  
SYSTEM SETTINGS FOR SIMULATIONS

Parameters	Values
Room size	5 m $\times$ 5 m $\times$ 5 m
Number of Transmitter/Receiver	1 $\times$ 1
Reflection coefficients ( $\alpha$ )	0.7
Transmitter FOV ( $\Phi_{1/2}$ )	45°
Receiver random rotation angles	0° to 360°
Receiver elevation angle	0° to 30°
Receiver FOV ( $\phi_{1/2}$ )	45°
SNR	from 15dB to 30dB
Collection area ( $A$ )	1 cm <sup>2</sup>
Modulation schemes	64 QAM
Number of subcarriers $N_f$	324
CP length $L_{CP}$	7
Pilot spacing $L_s$	5
OFDM symbols in one slot $N_s$	14
DC bias	7dB
Frequency spacing	30kHz

offline training dataset for the three InterpolateNet networks (LDS, MDS or HDS channels) consists of 100,000 channel samples with the SNR values for the environmental SNR range specified above, 95% for training and 5% for validation. Referring to the simulation settings given in Table. I, both  $\mathbf{h}_{LDS}$  and  $\mathbf{h}_{HDS}$  are assumed to be  $\mathbf{h}_{LDS} = 1e-4 * [6.4, 0.21930, 0.09676, 0.06175, 0.04517]$  and  $\mathbf{h}_{HDS} = 1e-4 * [5.5, 0.30126, 0.13441, 0.08609, 0.06310]$  respectively for this indoor scenario. Moreover, an InterpolateNet trained with HDS condition is implemented for comparison. We use MSE loss for training InterpolateNets and the detailed training hyper-parameters are given in Table. II.

TABLE II  
OFFLINE TRAINING HYPERPARAMETERS

Parameters	Values
Optimizer	Adam
Maximum epoch	100
Initial learning rate (lr)	0.0002
Drop period for lr	every 10
Drop factor for lr	0.3
Minibatch size	64
L2 regularization	$10^{-9}$

#### A. NMSE performance on randomly generated channels

We evaluate the NMSE performance of the proposed method on randomly generated channels over both SNR and time, to investigate the robustness property for practical implementations. The test channels are generated randomly according to Table. I.

Figure. 3a shows the NMSE performance over the SNR from 15dB to 30dB and each sample is averaged by 100,000 independent channel realizations. The proposed method is shown to have superior performance than other methods except for MMSE method. At 30dB SNR, the adaptive InterpolateNet achieves a NMSE of 0.5046 which is 0.0020 lower than that of HDS InterpolateNet. The MMSE method has a minimum NMSE value of 0.5001.

For the figure. 3b, the channel will alter among LDS, MDS and HDS for each 10 seconds and each sample is averaged over 100 independent channel realizations. Both the proposed method and the InterpolateNet trained with HDS condition outperform the LS estimate but are worse than MMSE method. The proposed method provides a better NMSE performance with a mean value of 0.5034, which is lower than 0.5052 for the InterpolateNet trained with HDS condition. Compared to the MMSE estimate with NMSE of 0.5012, the proposed solution does not require any actual channel information for online implementation resulting in poorer estimate performance and the NMSE variance of the proposed method is reasonably small over time.

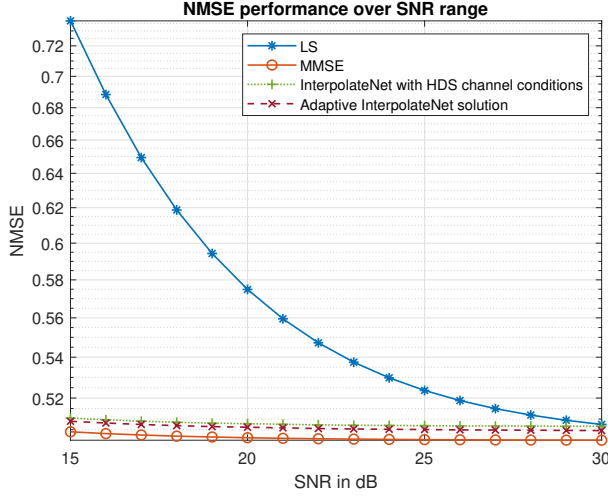
#### B. BER performance on randomly generated channels

We also evaluate the BER performance of each method on randomly generated channels over SNR. The test channels are also generated randomly according to Table. I.

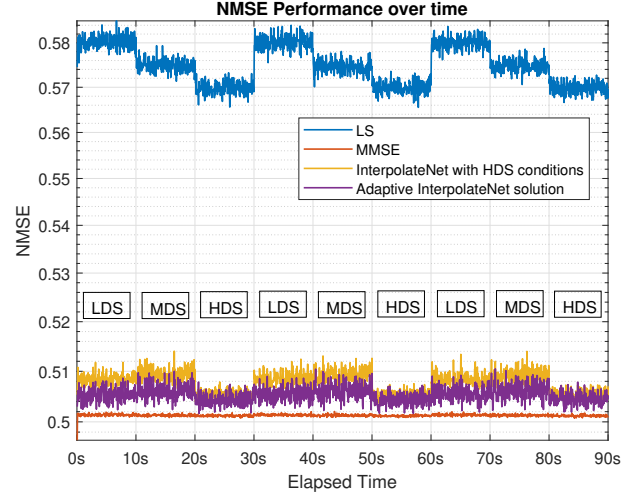
Figure. 4 shows the BER performance over the SNR from 15dB to 30dB and each sample is averaged by 100,000 independent channel realizations. The proposed method also outperforms other methods except for MMSE method. At 30dB SNR, the adaptive InterpolateNet achieves a BER of 4.8% while HDS InterpolateNet has a BER of 5.12%. The MMSE method has a minimum NMSE value of 2.7%. It should be noted that BER raise to 33.79% for optical receivers that directly demodulate the received signals. Replacing InterpolateNet with high-complexity neural networks should further improve both the NMSE and BER performance. This is because the neural network capacity is small due to the low complexity property of InterpolateNet and the deployed optical wireless channels are weakly frequency-selective type.

## V. CONCLUSION

This paper proposes an effective and low-complexity neural network solution to robustly estimate optical wireless channels, which are possible to be frequency-selective. Compared with conventional neural networks, the proposed method selects one suitable candidate neural network based on the prediction of another neural network on the channel to provide the most accurate prediction. From the simulation results, the proposed solution maintains a coherent performance over randomly-generated optical channels and achieves superior performance on both NMSE and BER than other methods which have no prior channel information known. Compared to the HDS InterpolateNet and the LS estimate, the adaptive solution achieves reductions in NMSE and BER of 1.04% and 1.5% for the HDS InterpolateNet, and 11.71% and 20% for the



(a) NMSE performance over SNR from 15dB to 30dB.



(b) NMSE performance over 90 seconds time with SNR fixed at 20dB.

Fig. 3. NMSE performance of LS, MMSE, InterpolateNet trained with HDS conditions and the proposed method.

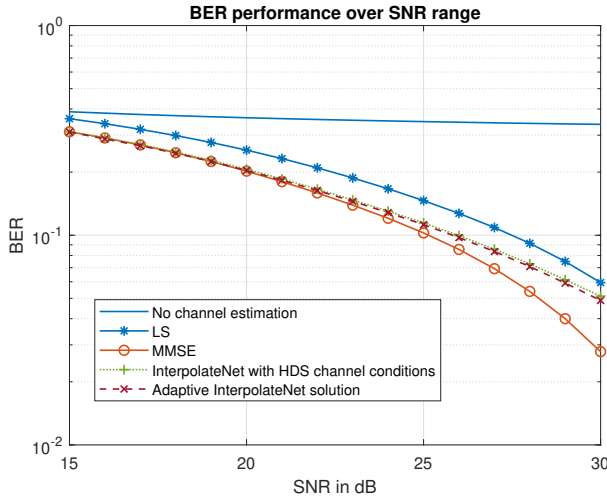


Fig. 4. BER performance of LS, MMSE, direct signal detection, InterpolateNet trained with HDS conditions and the proposed method over SNR from 15dB to 30dB.

LS estimate, respectively, at 20 dB SNR. Using the proposed solution does not require any actual channel information at the receiver end to precisely predict randomly-generated channels.

#### ACKNOWLEDGMENTS

This research is supported by EPSRC projects EP/X04047X/1 and EP/Y037243/1.

#### REFERENCES

- [1] C.-X. Wang, X. You, X. Gao, X. Zhu, Z. Li, C. Zhang, H. Wang, Y. Huang, Y. Chen, H. Haas *et al.*, "On the road to 6g: Visions, requirements, key technologies, and testbeds," *IEEE Communications Surveys & Tutorials*, vol. 25, no. 2, pp. 905–974, 2023.
- [2] X. You, C.-X. Wang, J. Huang, X. Gao, Z. Zhang, M. Wang, Y. Huang, C. Zhang, Y. Jiang, J. Wang *et al.*, "Towards 6g wireless communication networks: Vision, enabling technologies, and new paradigm shifts," *Science China Information Sciences*, vol. 64, pp. 1–74, 2021.
- [3] H. Ye, G. Y. Li, and B.-H. Juang, "Power of deep learning for channel estimation and signal detection in ofdm systems," *IEEE Wireless Communications Letters*, vol. 7, no. 1, pp. 114–117, 2017.
- [4] J. Gao, M. Hu, C. Zhong, G. Y. Li, and Z. Zhang, "An attention-aided deep learning framework for massive mimo channel estimation," *IEEE trans on wireless communications*, vol. 21, no. 3, pp. 1823–1835, 2021.
- [5] S. Ji and J. Thompson, "Robust machine learning for channel estimation with varying delay and doppler shift conditions," in *2023 IEEE 97th Vehicular Technology Conference (VTC2023-Spring)*. IEEE, 2023, pp. 1–5.
- [6] D. Luan and J. Thompson, "Attention based neural networks for wireless channel estimation," in *2022 IEEE 95th Vehicular Technology Conference (VTC2022-Spring)*. IEEE, 2022, pp. 1–5.
- [7] D. Luan and J. S. Thompson, "Channelformer: Attention based neural solution for wireless channel estimation and effective online training," *IEEE Transactions on Wireless Communications*, vol. 22, no. 10, pp. 6562–6577, 2023.
- [8] C. Gong and Z. Xu, "Channel estimation and signal detection for optical wireless scattering communication with inter-symbol interference," *IEEE Transactions on Wireless Communications*, vol. 14, no. 10, pp. 5326–5337, 2015.
- [9] H. Lu, M. Jiang, and J. Cheng, "Deep learning aided robust joint channel classification, channel estimation, and signal detection for underwater optical communication," *IEEE transactions on communications*, vol. 69, no. 4, pp. 2290–2303, 2020.
- [10] M. A. Amirabadi, M. H. Kahaei, S. A. Nezamhosseini, and V. T. Vakili, "Deep learning for channel estimation in fso communication system," *Optics Communications*, vol. 459, p. 124989, 2020.
- [11] A. Elfikky and Z. Rezki, "Symbol detection and channel estimation for space optical communications using neural network and autoencoder," *IEEE Transactions on Machine Learning in Communications and Networking*, vol. 2, pp. 110–128, 2023.
- [12] "Ieee standard for information technology–telecommunications and information exchange between systems local and metropolitan area networks–specific requirements part 11: Wireless lan medium access control (mac) and physical layer (phy) specifications amendment 6: Light communications," *IEEE Std 802.11bb*, pp. 1–37, 2023.
- [13] P. F. Mmbaga, J. Thompson, and H. Haas, "Performance analysis of indoor diffuse vlc mimo channels using angular diversity detectors," *Journal of Lightwave Technology*, vol. 34, no. 4, pp. 1254–1266, 2016.

- [14] J. R. Barry, J. M. Kahn, W. J. Krause, E. A. Lee, and D. G. Messerschmitt, "Simulation of multipath impulse response for indoor wireless optical channels," *IEEE journal on selected areas in communications*, vol. 11, no. 3, pp. 367–379, 1993.
- [15] P. Fahamuel, J. Thompson, and H. Haas, "Study, analysis and application of optical ofdm, single carrier (sc) and mimo in intensity modulation direct detection (im/dd)," 2013.
- [16] D. Luan and J. Thompson, "Low complexity channel estimation with neural network solutions," in *WSA 2021; 25th International ITG Workshop on Smart Antennas*. VDE, 2021, pp. 1–6.
- [17] —, "Achieving robust generalization for wireless channel estimation neural networks by designed training data," in *ICC 2023-IEEE International Conference on Communications*. IEEE, 2023, pp. 3462–3467.
- [18] H. Elgala, R. Mesleh, and H. Haas, "Practical considerations for indoor wireless optical system implementation using ofdm," in *2009 10th International Conference on Telecommunications*. IEEE, 2009, pp. 25–29.